NRIAG Journal of Astronomy and Geophysics (2015) 4, 134–146

National Research Institute of Astronomy and Geophysics

NRIAG Journal of Astronomy and Geophysics

www.elsevier.com/locate/nrjag

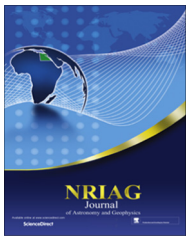

Delineating groundwater and subsurface structures by using 2D resistivity, gravity and 3D magnetic data interpretation around Cairo–Belbies Desert road, Egypt

Sultan Awad Sultan Araffa [a,*], Ahmed S. Helaly [b], Ashraf Khozium [a], Amir M.S. Lala [b], Shokry A. Soliman [c], Noha M. Hassan [d]

[a] *National Research Institute of Astronomy and Geophysics, Helwan, 11722 Cairo, Egypt*
[b] *Faculty of Science, Ain Shams University, Egypt*
[c] *Petroleum Research Institute, Egypt*
[d] *Faculty of Science, Menoufiya University, Egypt*

Received 6 February 2015; revised 3 June 2015; accepted 25 June 2015
Available online 8 July 2015

KEYWORDS

Gravity;
Magnetic;
Resistivity;
Dipole–dipole

Abstract Geophysical tools such as magnetic, gravity and electric resistivity have been used to delineate subsurface structures, groundwater aquifer around Cairo–Belbies Desert road. A dipole–dipole section was measured at the central part of the study area with 2100 m length and electrode spacing 50 m for greater penetration depth. The results of the inverse resistivity data indicate that the study area includes two groundwater aquifers at different depths. The shallow aquifer water is near the surface and the deep aquifer lies at depth of about 115 m and exhibits low resistivity values ranging from 20 to 100 ohm m.

One hundred and fifty-two gravity stations were measured using Autograv gravimeter (CG3), different gravity corrections (drift, elevation and latitude corrections) were applied. The corrected data represented by Bouguer anomaly map were filtered into regional and residual gravity anomaly maps. The residual gravity map indicates that the area is dissected by many faults with NW-SE, N-S, E-W and NE-SW trends.

One hundred and fifty-three ground magnetic measurements are collected using two Proton magnetometers (Envimag). The corrected magnetic data are represented by total magnetic intensity map that was reduced to the magnetic pole. 3D magnetic modeling was applied to detect the depth

* Corresponding author.
E-mail address: sultan_awad@yahoo.com (S.A.S. Araffa).

Peer review under responsibility of National Research Institute of Astronomy and Geophysics.

ELSEVIER Production and hosting by Elsevier

http://dx.doi.org/10.1016/j.nrjag.2015.06.004

of basaltic sheet and basement complex. The results indicated that the elevation of upper surface of basalt is ranging from 148 to −153 m and the elevation of lower surface of basalt is ranging from 148 to 269 m.

1. Introduction

The study area lies at the northeastern part of Greater Cairo and located from the western part by urban and cultivated areas, and bounded by latitudes 30°15′ & 30°19′N and longitudes 31°23′ & 31°30′E (Fig. 1). The study area includes large reclamation areas at the central part, which need underground water for irrigation and cultivation applications where the source of the River Nile water is far and costing. The technique of the integrated geophysical interpretation for groundwater exploration was used by different authors such as Hassanen et al. (2001), Sultan and Mohamed (2000), Santos et al. (2006) and Araffa, 2013 used 3D VES inversion and magnetic data for delineating groundwater aquifer near the study area. In the present work, the author uses 2D resistivity data of the dipole dipole configuration for the geoelectrical technique instead of the Shlumberger configuration, where the dipole dipole section estimates the upper and lower surfaces of the basaltic layer and the top surface of the deep groundwater aquifer.

1.1. Geology of the area

The surface geology and stratigraphic description of the study area were studied in detail by geological survey of Egypt (EGSMA, 1998), through fieldwork trips and Inshas borehole drilled at the western part of the study area (Figs. 2 and 3). The surface geology is composed of different geological units which belong to Quaternary and Tertiary deposits. The Quaternary deposits is represented by sand sheet cover the western part of the study area of Holocene, and the Pleistocene is represented by two Formations, the first is Inshas Formation which consists of cross-bedded sand intercalated with Nile mud and silt. The second formation is Bilbies Formation, which consists of medium to coarse grained sand with plant roots, intercalated with flint, chert and clay, and cover the most part of the study area. The Tertiary deposits is represented by Hommath Formation, which consists of sandy limestone, sandstone and sandy marl of Middle Miocene deposits and covers the southeastern part of the study area.

The subsurface stratigraphy was described through Inshas borehole drilled in the western part of the area by Geological Survey of Egypt (EGSMA, 1998) of depth 202 m and elevation 52.6 m USL, where the stratigraphic column consists of Quaternary, Middle Miocene and Oligocene deposits. The Quaternary deposits is represented by sand sheet, the Middle Miocene is represented by Hommath Formation but the Oligocene deposits composed of Basaltic sheet which, lies at depths of 113.5 m for the top and 162.2 m for the bottom surfaces of basalt (elevation of upper and lower surfaces of basalt is −60.9 and −109.6 m) and the results and tests of this basaltic sheet indicate that the top and bottom were altered and fractured. The second Formation of the Oligocene is represented by Gabal Ahmar Formation, which consists of sand and sandstone. The results of Inshas borehole indicate also,

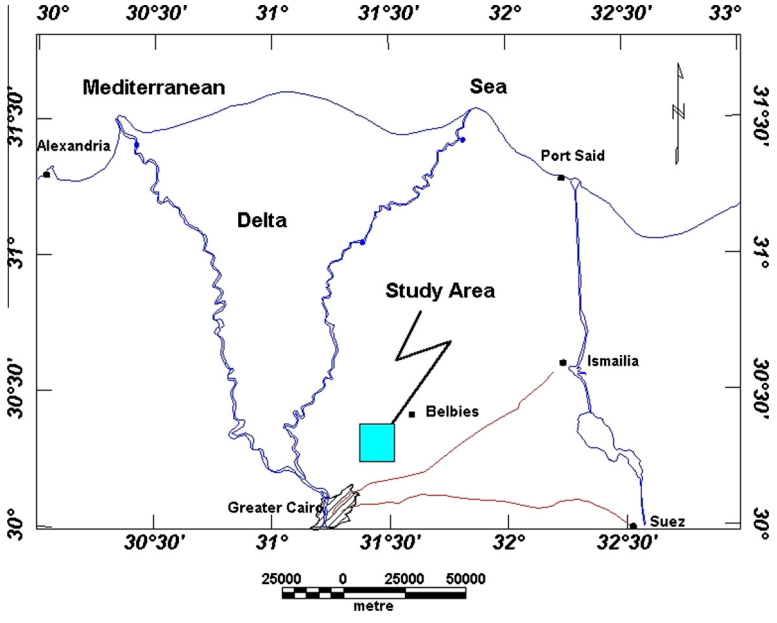

Figure 1 Location map of the study area.

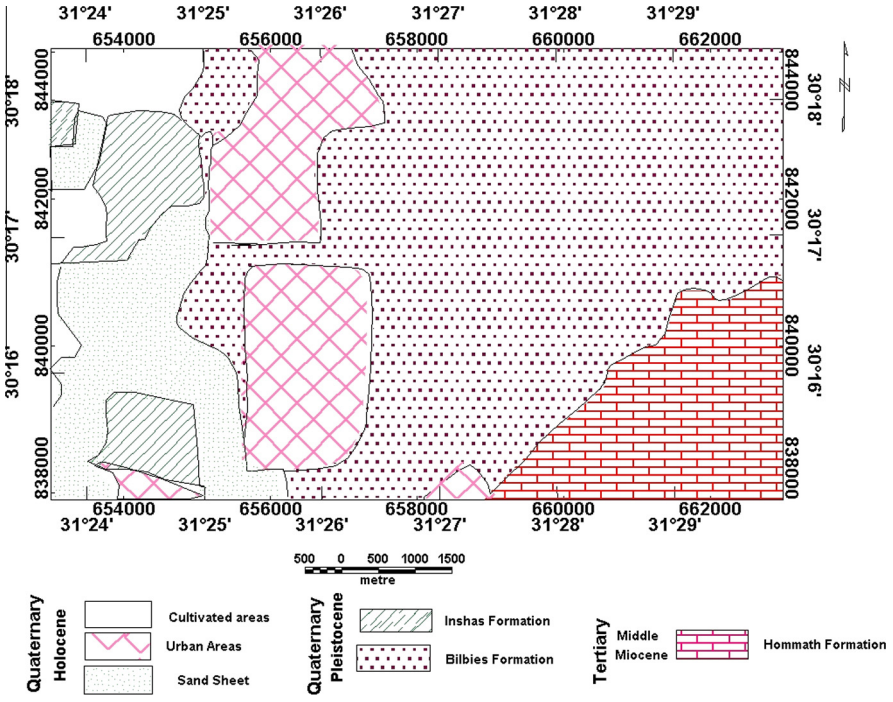

Figure 2 Simplified geological map of the study area (modified after EGSMA, 1997).

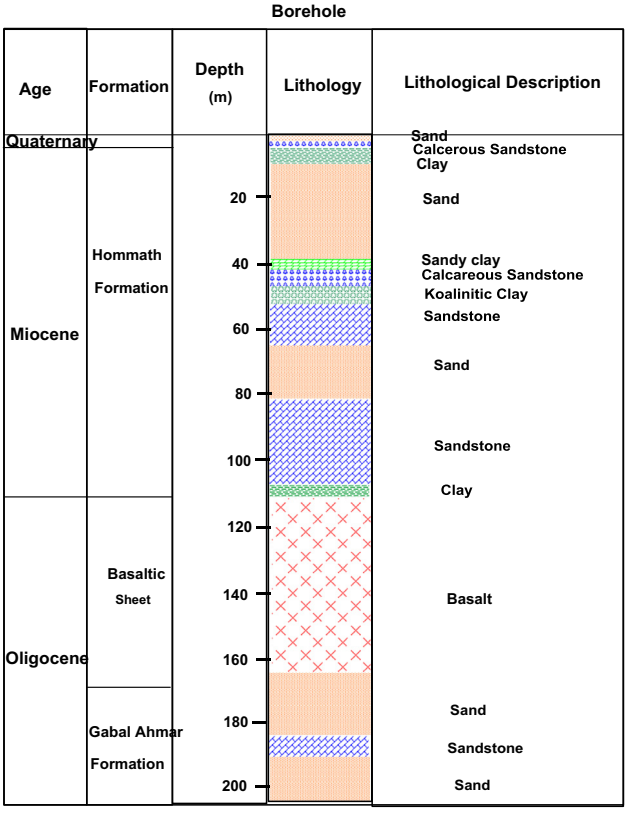

Figure 3 The stratigraphy of the study area; described from Inshas borehole.

the area contains two aquifers for groundwater, the first is Miocene aquifer above basaltic sheet and the second is Gabal Ahmar aquifer underlying basaltic sheet (Fig. 3).

2. Geophysical measurements and Interpretation

2.1. The geoelectrical measurements and interpretation

Geoelectrical measurements represented in the present study by dipole–dipole resistivity technique have been carried out along profile A-A′ (Fig. 4) lies at the central part of reclamation zone. The zone of total length 2100 m needs to the groundwater for irrigation and cultivation. For the dipole dipole configuration, the two current electrodes (AB) are kept fixed while the potential electrodes (MN) are moved from n = 1–7 collinearly to the current ones, then AB is moved to the next electrode and so on until the end of the profile. The spacing between current electrodes and potential electrodes is a multiple of the electrode spacing (a). The depth of penetration is a function of the distance a (Edwards, 1977; Loke and Barker, 1996). In the present study, the electrode spacing (a) is 50 m in order to investigate shallow and deep groundwater aquifers and the subsurface stratigraphic sequence. The measurements have been carried out using a SYSCAL – R2, resistivity – meter is fully automatic equipment designed for DC electrical exploration. The dipole–dipole section A-A′ (Fig. 5) is inverted using the RESINV2D software which produces an image of the electrical resistivity distribution in the subsurface based on a regularization algorithm (Loke and Barker, 1996). The calculated model shows the different stratigraphic units corresponding to Quaternary, Miocene and Oligocene deposits. The dipole dipole section exhibits different variation in the resistivity values range from 20 to 500 Ohm m, corresponding to lithological units and water content. The shallow part of the section is occupied by moderate to high resistivity values corresponding to Quaternary and Hommath Formation of Middle Miocene deposits. These deposits overlay basaltic sheet which exhibit high resistivity values,

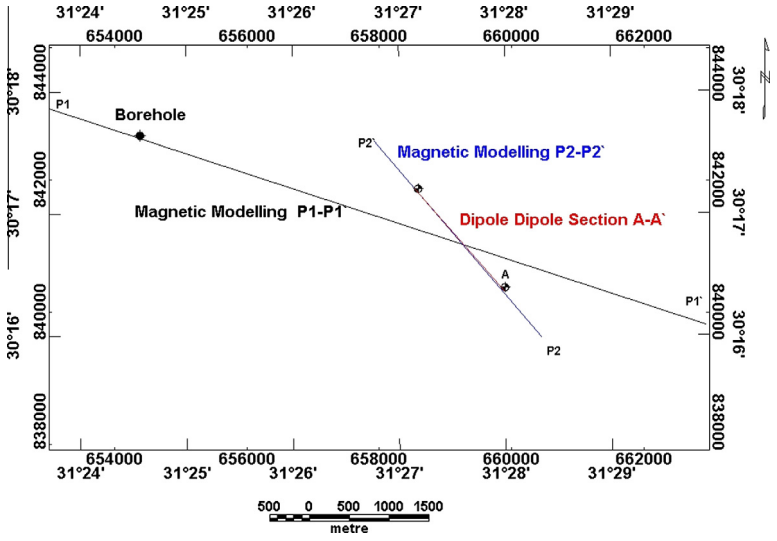

Figure 4 Location map of the geophysical profiles.

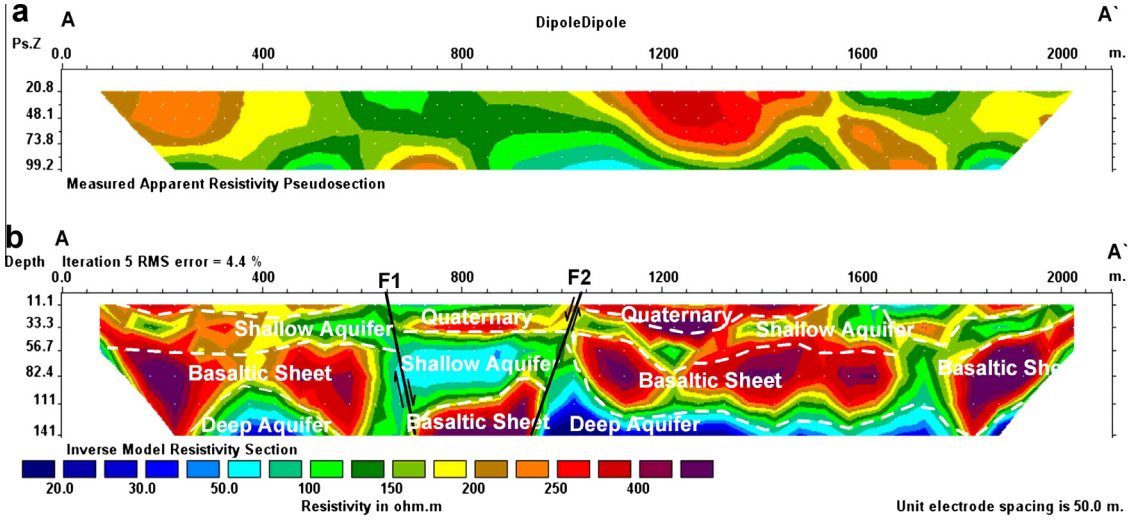

Figure 5 Dipole dipole section along profile A-A′.

the upper surface of the basaltic layer at depths about 40 m except the part near the center where the depth is about 135. This part was dissected by two normal faults (F1 and F2). The basaltic sheet overlays the deposits of Gabal Ahmar Formation of Oligocene deposits, which is the main aquifer in the study area and exhibits low resistivity values due to the sand and sandstone of this Formation saturated with groundwater. The depth to the main aquifer is about 115 m at the central part of the section and the shallow aquifer appears at the central and the end part of the section. The author used the relation between the electrical resistivity and porosity to define the porosity percentage through the dipole dipole profile. Also, this technique has been used before by Sultan et al. (2007). Archie (1942) proposed the following relationship between bulk (σ_b) and fluid (σ_f) conductivities:

$$\sigma_b = a\sigma_f\varphi^m \tag{1}$$

or

$$1/F = a\varphi^m \tag{2}$$

where a and m are parameters that are assumed constants for a certain type of rock, φ is the porosity and F is the formation factor. Eq. (1) assumes that the surface conduction is negligible when compared with electrolyte conduction. If this is not the case, Eq. (1) has to be modified to include those effects. Waxman and Smits (1968) proposed the first model shaly sand formations; assuming that clay particles contributing exchange cations to the electrolyte increase the conductivity of the formation. The Waxman and Smits (1968) model is expressed by

$$\sigma_b = \varphi^m(\sigma_f + BQ_v) \tag{3}$$

$$B = 4.6(1 - 0.6e^{-\sigma f/1.3}). \tag{4}$$

Q_v is the clay charge contribution per unit pore volume and is expressed in meq ml^{-1}. Sen et al. (1988) proposed an empirical law relating porosity with bulk conductivity,

$$\sigma_b = \varphi^m[(\sigma_f + \mu DLm_sQ_v/(1 + CQ_v/\sigma_f)] + EQ_v \tag{5}$$

where Q_v is the clay charge contribution per unit pore volume and is expressed in meq/ml, μDL is the mobility of the ions and

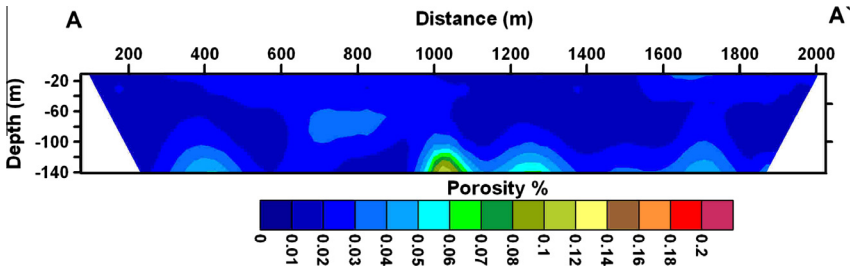

Figure 6 Porosity percentage along profile A-A′.

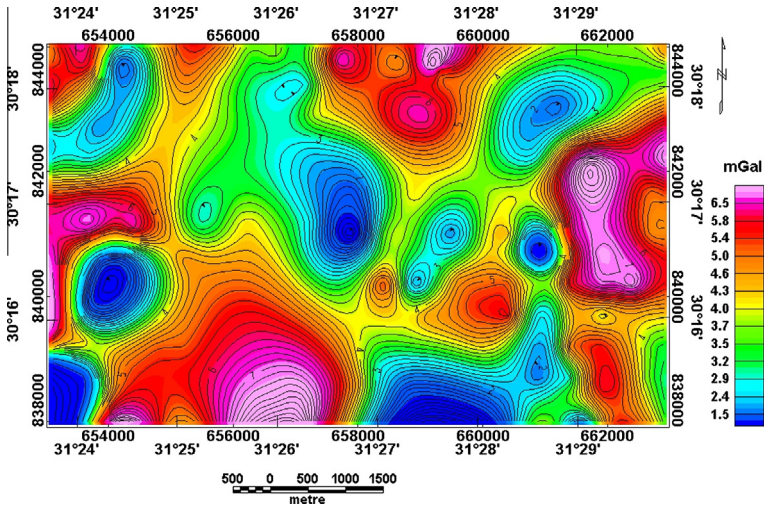

Figure 7 Bouguer anomaly map of the study area.

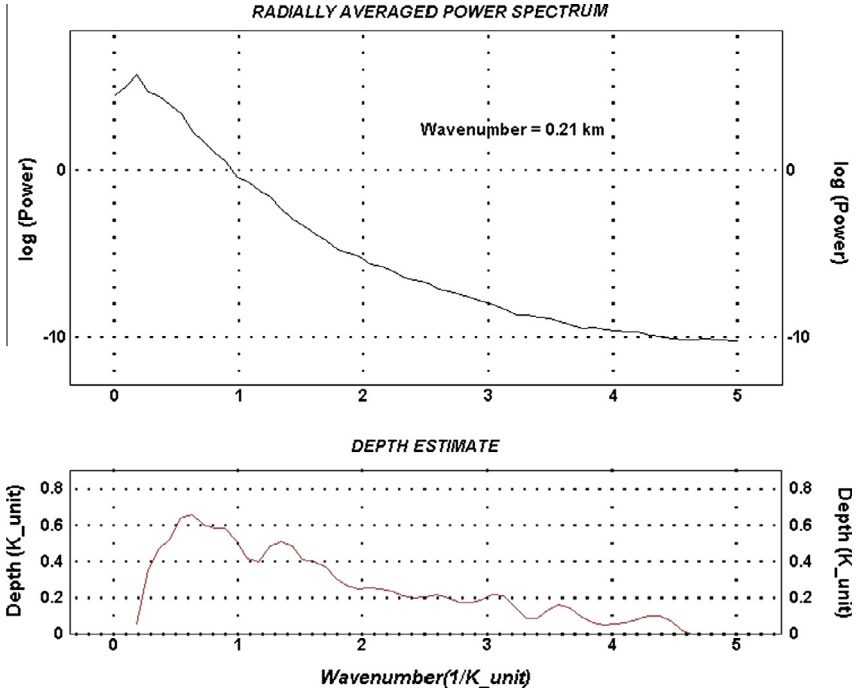

Figure 8 Radially averaged power spectrum.

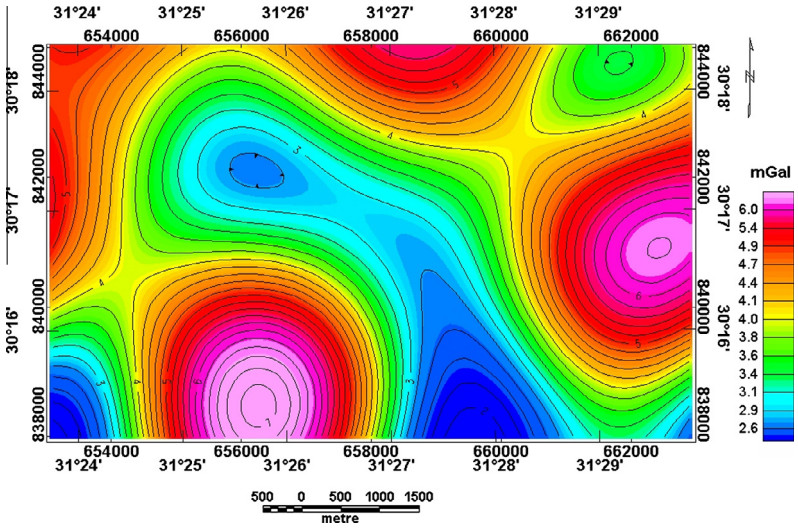

Figure 9 Regional gravity anomaly.

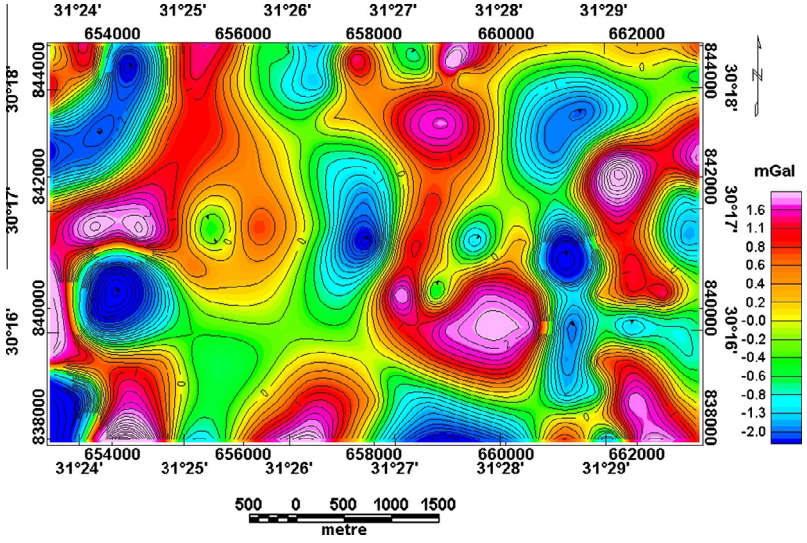

Figure 10 Residual gravity anomaly.

m_s is a surface tortuosity factor. C is a constant that depends on rock geometry and the effective mobility of cations near the surface (Sen et al. 1988). They found that their core data could be well fitted with $\mu DLm_s = 1.93 \times m\mathrm{Sl\,mol^{-1}}$, $CQv = 0.7$ S, $EQv \approx 0$, and $m \approx 2$. In the present study the water aquifer in the area is represented by Gabal Ahmar Formation which is composed of essential from sand and sandstone with free clay, where the $Qv = 0$. Then Eq. (5) becomes

$$\sigma_b = \varphi^2 \sigma_f \tag{6}$$

Thus, these values are adopted in this work. The fluid conductivity is measured at the Inshas borehole drilled in the area, where the result of the fluid conductivity is 12.5 mS/m. The calculations have been carried out for the dipole dipole section using the conductivity values for this section as the bulk conductivity in Eq. (6). The results suggest that the dipole dipole section exhibits porosity with values ranging from 0% to 12%. The highest values of porosity (ranging from 4% to 12%) are concentrated in the zone where the water aquifer is represented by sand and sandstone of Gabal Ahmar Formation at the central part of the section through the depth ranged from 115 to 141.5 m, the Miocene deposits (Hommath Formation) reveals porosity about 4% but the basaltic sheet is very low porosity about 0% (Fig. 6).

2.2. The gravity measurements and interpretation

One hundred and fifty-two gravity stations have been measured to represent a grid of 500 × 500 m. for the accessible sites to cover the study area. The gravity data have been measured by using an automatic gravity meter made by Scintrex (CG-3 Autograv) with a resolution of 0.01 mGal. Different corrections have been applied to the raw data, such as drift, tide, latitude, free-air and Bouguer corrections. The terrain correction is not carried out, where the area is more or less flat.

Bouguer anomaly values have been grided and contoured by using Geosoft programs Oasis Montaj (2007), to produce the Bouguer anomaly map (Fig. 7), which shows different high and low anomalous values through the surveyed area. High and low pass filters with a cutoff wave number of 0.21 km^{-1} (Fig. 8), have been applied to the Bouguer anomaly map in order to calculate the regional and residual maps. The regional gravity map exhibits a low gravity anomaly at the center of the area trending NW-SE (Fig. 9), but the residual gravity map (Fig. 10) shows different trends for the high and low local gravity anomalies.

The interpretation of the gravity data has been carried out on the residual gravity anomaly map to delineate the structural fault elements, which dissect the study area. The fault elements cover most of the study area; having the NE-SW, NW-SE, N-S and E-W trends (Fig. 11). The interpreted faults F1 and F2, which are located at the central part of the area and lie at the dipole dipole section, are confirmed through the interpretation of the resistivity data.

2.3. Magnetic measurements and interpretation

A ground magnetic survey has been carried out at same stations of the gravity measurements of the area under study. The total intensity magnetic field measurements have been carried out with two Envimag Proton magnetometers made by Scintrex Company in Canada with one 1 nT sensitivity. The values of the magnetic stations were corrected for diurnal variations and IGRF corrections. The diurnal variations of the earth's magnetic field may, sometimes, have amplitudes greater than 10 nT. These must, therefore, be taken into consideration in processing the data through the survey. Two

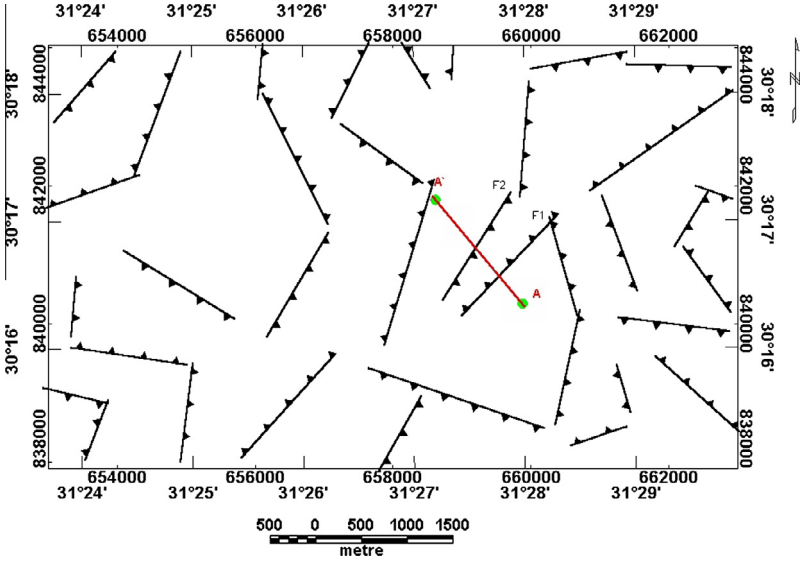

Figure 11 Fault elements dissecting the area from gravity interpretation.

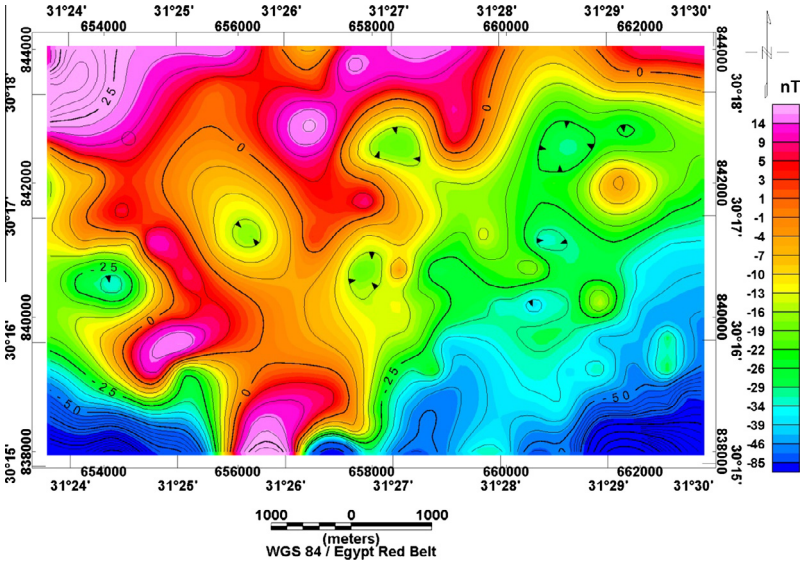

Figure 12 Total intensity magnetic map.

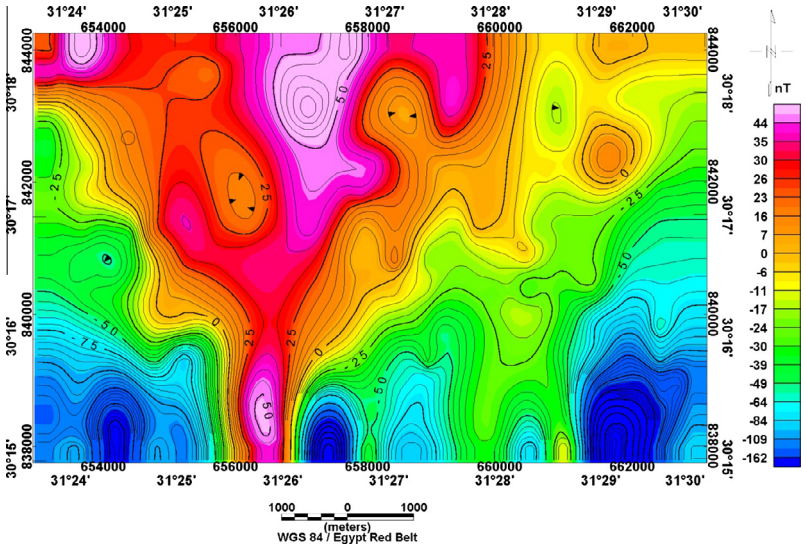

Figure 13 Total intensity magnetic map reduced to the pole.

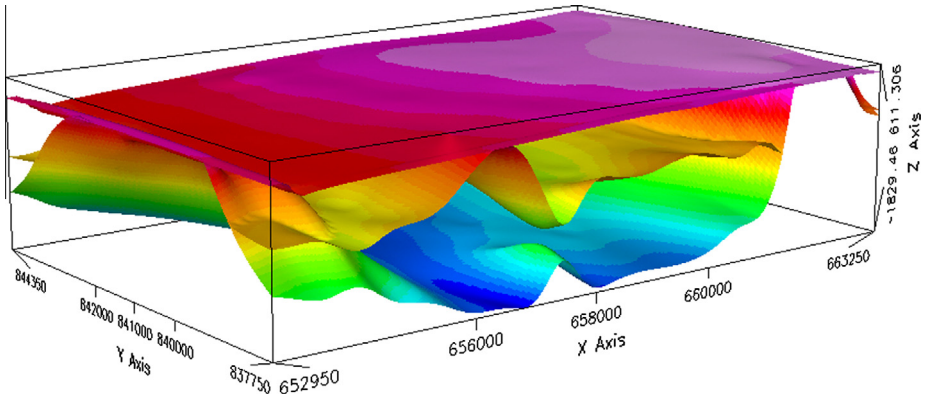

Figure 14 Output of GM-SYS 3D magnetic modeling.

instruments have been used, one of them in a base station, recording the data every one-minute and the other one has been used as a field instrument to carry out the measurements at the stations along the profiles. The corrected magnetic values have been gridded and contoured using Geosoft programs Oasis Montaj (2007). The resulting picture represents a preliminary total intensity magnetic map (Fig. 12). The total intensity magnetic map has been reduced to the north magnetic pole, where the magnetic fields created by geological bodies are distorted by the inclination of the earth's field. As a consequence of those distortion effects, the peak of the anomalies is shifted from the centers of the magnetized bodies, making difficult to determine correctly the shapes and locations of these magnetized bodies. This mathematical procedure was first described by Baranov (1957). The total intensity magnetic map reduced to the pole (Fig. 13) exhibits high magnetic anomaly is occupying the northern part and extends to the central part of the area, but the southern part is occupied by low magnetic anomalies.

2.3.1. 3D magnetic modeling

3D modeling is a new technique to estimate the elevation of upper and lower surfaces of basalt and also, the elevation of basement rocks in the study area by using GMSYS-3D software. GMSYS-3D software, which is one programs of the geosoftw (Oasis Montaj, 2007). GMSYS-3D is a 3D gravity and magnetic modeling package for surface-oriented models. A model is defined by a number of stacked surface grids with density, susceptibility, and remnant magnetization-distributions specified for the layer below each surface. The authors used susceptibility 7650 micro CGS units for basaltic sheet 32 micro CGS for Miocene deposits and 200 micro CGS units for Gabal Ahmar Formation (Araffa, 2013), after applying 20 iteration for the running software (Oasis Montaj, 2007). The output results indicate that there are coincidence between the observed magnetic data (RTP) and calculated magnetic data (RTP). Also, the results of 3D modeling indicated that the elevation of upper surface of basalt is ranging from −153 to 148 m from sea level and the elevation

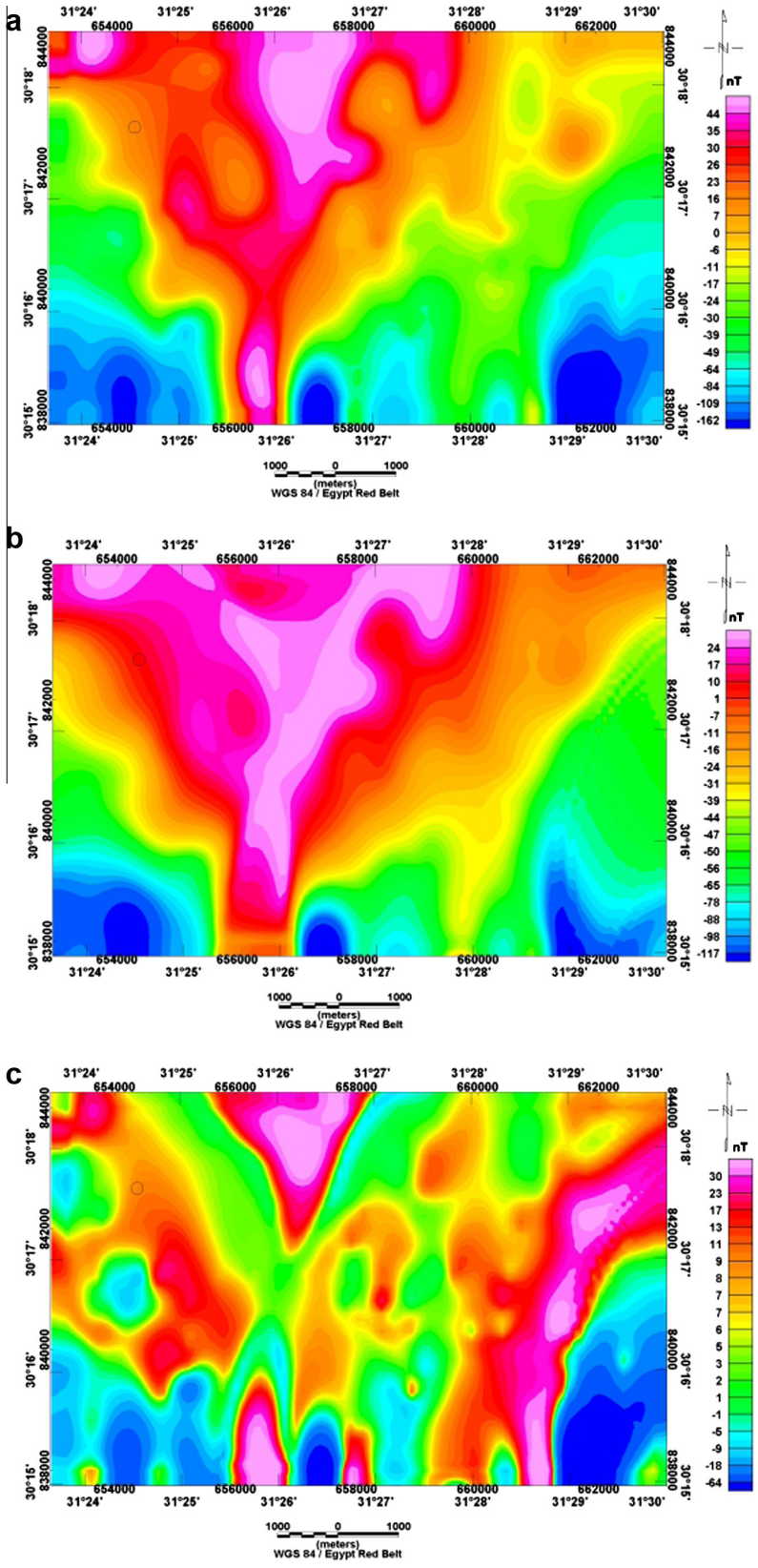

Figure 15 3D magnetic modeling data for upper and lower basaltic surfaces, (A) observed RTP map, (B) calculated RTP map, (C) error between observed and calculated, where the fig. indicates the compatible between observed and calculated magnetic data.

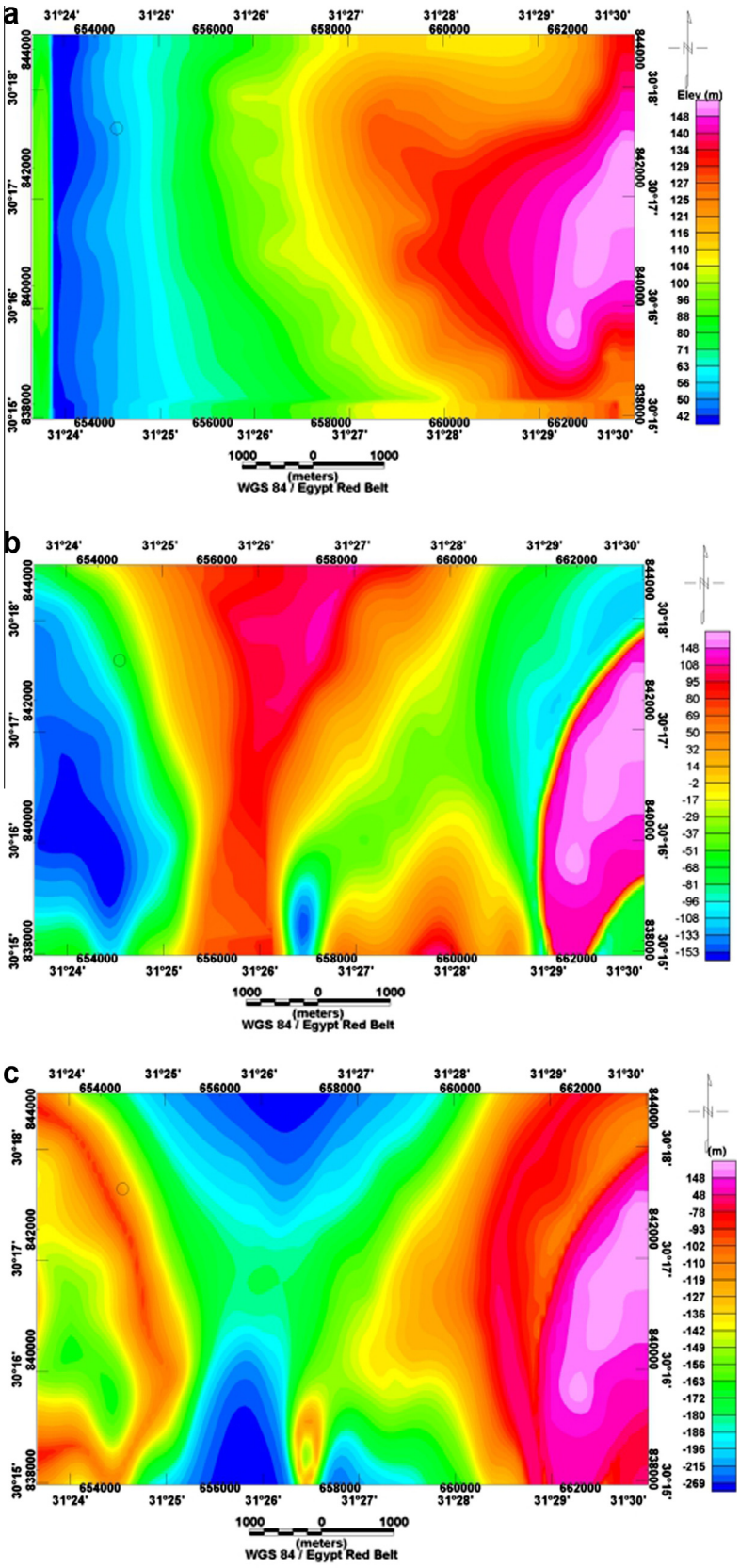

Figure 16 Results of 3D magnetic modeling, (a) topography, (b) elevation of upper surface of basalt, (c) elevation of lower surface of basalt from sea level.

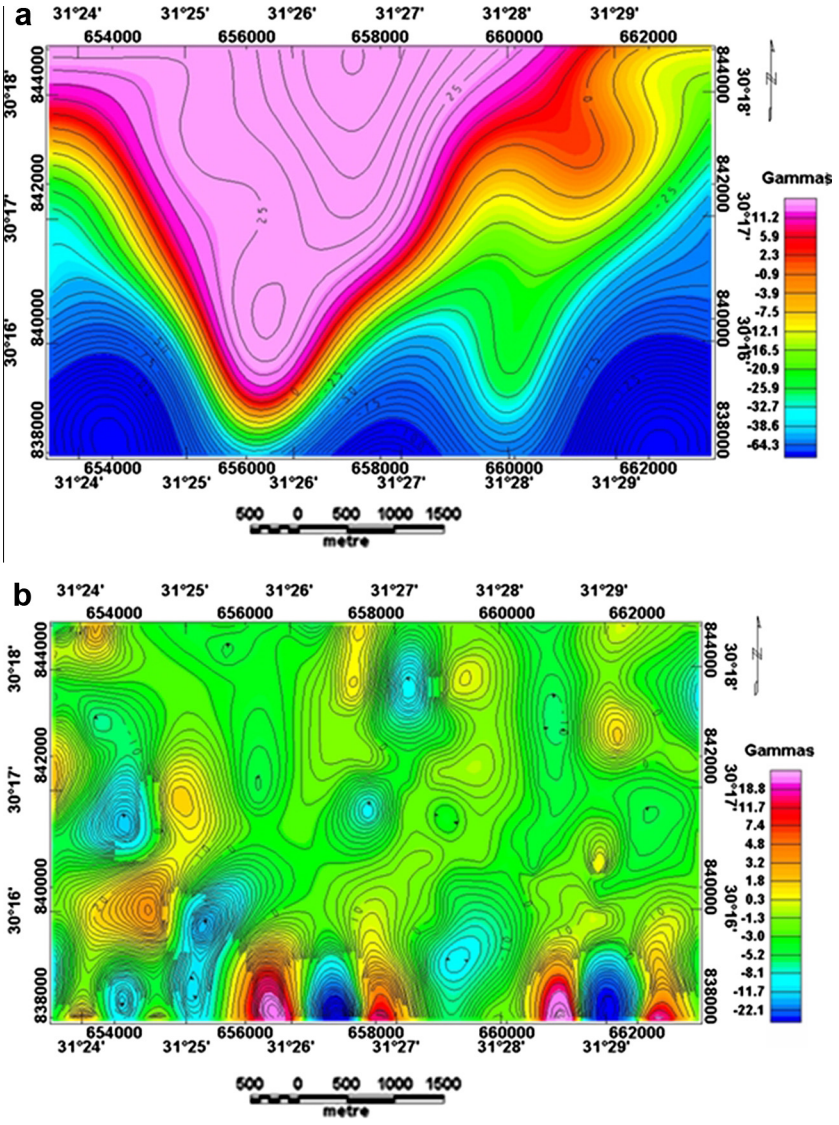

Figure 17 (a) Regional total intensity magnetic map reduced to the pole, (b) residual total intensity magnetic map reduced to the pole.

of lower surface of basalt is ranging from −269 to 148 m from sea level which are compatible with results of the Inshas borehole drilled in the study area (Figs. 14–16).

2.3.2. Magnetic data separation

The total intensity magnetic map reduced to the pole is filtered to construct the regional and residual magnetic map (Fig. 17) using the same technique, which is used in gravity separation.

2.3.3. 2D magnetic modeling

The residual total intensity magnetic map is used for applying 2D magnetic modeling to determine the depth of the upper surface of basaltic sheet. There are several computer programs available to calculate the magnetic response of the subsurface geological sections. In the present study, the GM-sys program produced by the Northwest Geophysical Associates Inc. USA (2007) was used. Two magnetic profiles crossing perpendicularly the magnetic anomalies and using magnetic susceptibility of 0.00765 cgs unit for the basaltic sheet are investigated. One of them is passing through the Inshas borehole where the depth of the upper surface of the basaltic sheet is estimated at 113.5. The second profile is passing through the dipole section to detect the upper surface of the basaltic sheet. The intersection point of the two profiles has been taken as a reference point through the modeling process of the second profile. The magnetic model along profile P1-P1′ (Fig. 18) suggests that the depth of the upper surface of the basaltic sheet varies along the profile, being deeper (about 195 m) at the end part of the profile. The basaltic sheet is shallower at 2 km before the end of the profile at a depth of 40 m. The magnetic model along profile P2-P2′ (Fig. 19) exhibits different variation for the upper and lower surfaces of the basaltic sheet. The beginning and end parts of the profile reveal deep depths for the upper surface of the basaltic sheet about 150 m but the central part exhibits shallow depth about 50 m.

3. Discussion

The results of geological and geophysical data in the study area are compatible with each other where, the depth of upper and

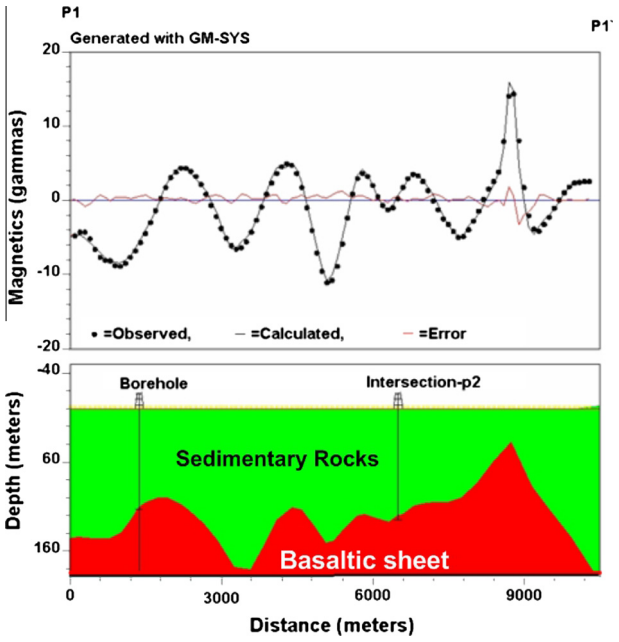

Figure 18 2D magnetic modeling along profile P1-P1′.

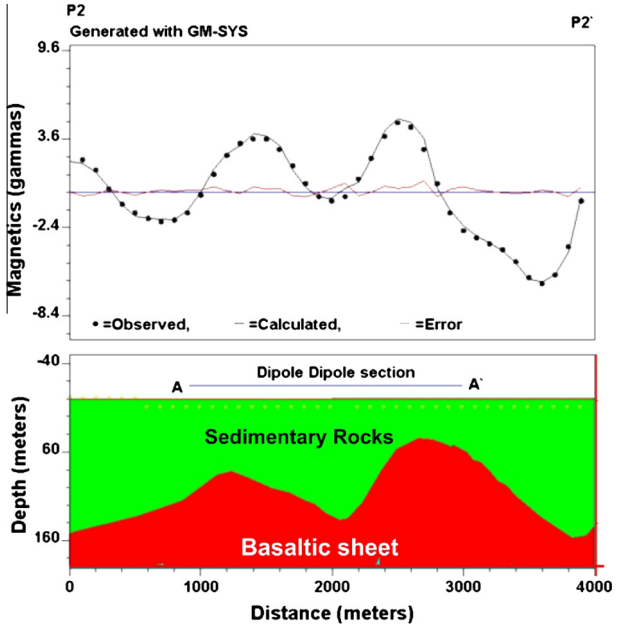

Figure 19 2D magnetic modeling along profile P2-P2′.

lower surfaces of basaltic sheet in Inshas borehole is 113.5 and 162.2 m (elevation of upper and lower surfaces of basalt are −60.9 and −109.6 m) are similar to the elevation of upper and lower of basalt from the interpretation from 3D magnetic modeling about −57 and −106 m, the depth of upper surface of basalt from interpretation of 2D magnetic modeling also about 112 m is compatible with the depth of upper surface of basalt from Inshas borehole data. The interpretation of dipole dipole section indicates that the area of the study contains two aquifers, the first is Miocene aquifer and the lower aquifer is Gabal Al ahmar Formation which are conformed to result of Inshas borehole. The interpretation of gravity data indicates that the study area is dissected by different fault elements, two of these faults F1 and F2 are indicted in the 2-D resistivity section and also in 2D magnetic modeling. There is a good agreement between the results of the 2D resistivity, gravity, magnetic modeling and those obtained from the Inshas borehole. The quite difference between the depth values of the basaltic sheet from magnetic modeling and those obtained from the 2D resistivity interpretation is due to the fact that the upper and lower parts of the basaltic sheet were altered and fractured, then they saturated with groundwater. For this reason, the resistivity values are decreased and the thickness of the basaltic sheet detected from the resistivity interpretation seems less than the thickness from magnetic modeling. The different values between the results for the two techniques range from 10 to 20 m, which are in good agreement.

4. Conclusion

From the results of the interpretation of the 2D resistivity dipole–dipole, gravity, and magnetic data, we conclude that the area is affected by different fault elements of NW-SE, NE-SW, N-S and E-W trends, reflecting the distribution of the basaltic sheet. The study area contains two aquifers, one of them is shallower and the second is deeper. The deep aquifer represents the main aquifer in the study area, the main aquifer lies at depth about 110 m and exhibits high porosity about 13%. The basaltic sheet exhibits variation of the depth for the upper and lower surfaces, where elevation of the upper surface ranges from 148 to −153 m but the elevation of the lower surface ranges from 148 to −269 m. The main aquifer is more shallow under the part which exhibits high magnetic anomalous where the basaltic sheet is shallower and represented as impervious layer for the aquifer.

References

Araffa, S.A.S., 2013. Delineation of groundwater aquifer and subsurface structures on north Cairo, Egypt, using integrated interpretation of magnetic, gravity and geoelectrical data. Int. J. Geophy. 192 (1), 94–112.

Archie, G.E., 1942. The electrical resistivity log as an aid in determining some reservoir characteristics. Petr. Tech. 1, 55–62.

Baranov, V., 1957. A new method for interpretation of aeromagnetic maps: pseudo-gravimetric anomalies. Geophysics 22, 359–383.

Edwards, L.S., 1977. A modified pseudosection for resistivity and induced polarization. Geophysics 42, 1020–1036.

Geological Survey of Egypt (EGSMA), 1998. Geology of Inshas Area, Geol. Surv. of Egypt, internal report.

Geosoftw Program (Oasis Montaj), 2007. Geosoft mapping and application system Inc, Suit 500, Richmond St. West Toronto, ON Canada N5SIV6.

Hassanen, A.Gh., Sultan, S.A., Mohamed, B.S., 2001. Integrated Geophysical Interpretation for groundwater exploration at Nukhl Area, Central Sinai. Bul. National Res. Inst. Astronomy Geophys., Ser. B 2001, 283–298.

Loke, M.H., Barker, R.D., 1996. Rapid least-squares inversion of apparent resistivity pseudosections by a quasi-Newton method. Geophys. Prospect. 44, 131–152.

Santos, F.A.M., Sultan, S.A., Patrıcia, R., El Sorady, A.L., 2006. Joint inversion of gravity and geoelectrical data for groundwater and structural investigation: application to the northwestern part of Sinai, Egypt, geophys. J. Int. 165, 705–718.

Sen, P.N., Goode, P.A., Sibbit, A., 1988. Electrical conduction in clay bearing sandstones at low and high salinities. J. Appl. Phys. 63 (10), 4832–4840.

Sultan, S.A., Mohamed, B.S., 2000. Geophysical Investigation for Groundwater at Wadi Ghuwaybah,- Northeastern Part of Eastern Desert, Egypt. Annals Geol. Surv. Egypt XXIII, 901–918.

Sultan, S.A., Mansour, S.A., Fernando, M.Santos., 2007. Hydro-geophysical Investigation in Ain Mousa area, Northern part of Mokattam City, Cairo, Egypt. Bul. Environ. Geol. Eng. http://dx.doi.org/10.1007/s10064-007-0107-0.

Waxman, M.H., Smits, L.J.M., 1968. Electrical conductivities in oil-bearing shaly sands. Soc. Pet. Eng. J. 8, 107–122.